JCTC Journal of Chemical Theory and Computation
Article
Cite This: J. Chem. Theory Comput. 2019, 15, 348−356
pubs.acs.org/JCTC

Generalized Hartree−Fock with Nonperturbative Treatment of Strong Magnetic Fields: Application to Molecular Spin Phase Transitions

Shichao Sun, David B. Williams-Young, Torin F. Stetina, and Xiaosong Li*

Department of Chemistry, University of Washington, Seattle, Washington 98195, United States

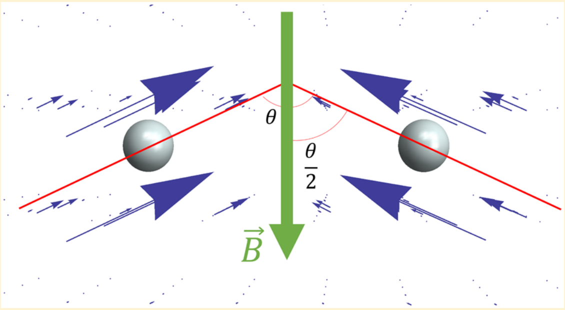

ABSTRACT: In this work, we present a framework of an ab initio variational approach to effectively explore electronic spin phase transitions in molecular systems inside of a homogeneous magnetic field. In order to capture this phenomenon, the complex generalized Hartree−Fock ($\mathbb{C}$-GHF) method is used in the spinor formalism with London orbitals. Recursive algorithms for computing the one- and two-electron integrals of London orbitals are also provided. A Pauli matrix representation of the $\mathbb{C}$-GHF method is introduced to separate spin contributions from the scalar part of the Fock matrix. Next, spin phase transitions in two different molecular systems are investigated in the presence of a strong magnetic field. Noncollinear spin configurations are observed during the spin phase transitions in H_2 and a dichromium complex, $[(H_3N)_4Cr(OH)_2Cr(NH_3)_4]^{4+}$, with an increase in magnetic field strength. The competing driving forces of exchange coupling and the spin Zeeman effect have been shown to govern the spin phase transition and its transition rate. Additionally, the energetic contributions of the spin Zeeman, orbital Zeeman, and diamagnetic terms to the potential energy surface are also analyzed.

1. INTRODUCTION

Electron spin is a fundamental physical property that is important to a wide array of science and technological applications such as energy storage, quantum computing, and chemical catalysis. An atomic or molecular system has a spin-dependent many-electron response that can be perturbed by an external electromagnetic field. Although effective model Hamiltonians with perturbative treatments of external fields[1−4] have their merits, they are limited in their description of spin-dependent processes in the strong perturbation limit. While molecular response to external electric fields has been a subject of extensive theoretical work, computational frameworks for modeling finite magnetic field effects have been lagging behind mainly due to three challenges; the gauge-origin problem, spin noncollinearity, and the necessity of complex arithmetic.

For many-atom systems, electronic structure calculations in the presence of electromagnetic fields become dependent on the choice of the gauge-origin, mainly due to the basis set incompleteness of Gaussian-type orbitals.[5−12] Among various approaches to correct for the gauge-origin problem, electronic structure methods using London-type orbitals[13,14] provide the most satisfactory solution.[15−21] London orbitals are constructed from conventional atomic orbitals (AOs) dressed by a complex phase factor that depends on the external vector potential and are considered physically appropriate for modeling chemical systems in an external magnetic field.[5]

In the nonperturbative limit, such as in the presence of a strong magnetic field, variational treatment of the electronic structure using London orbitals is required.[22−24] For this purpose, Helgaker and co-workers have made algorithmic advances for evaluating one- and two-electron integrals using London orbitals and applied a variational approach to study molecules in strong magnetic fields within the spin-collinear framework at the level of Hartree−Fock,[25,26] coupled cluster,[27] configuration interaction,[28] density functional theory, and current density functional theory.[29−31] While the electronic characteristics of spin states in a magnetic field can be obtained using a variational spin-collinear method, the spin phase transition process, e.g., from singlet to triplet, driven by a static magnetic field requires a spin-noncollinear treatment.

It is well-known that certain symmetry breaking, such as an external static magnetic field breaking time reversal symmetry and geometric frustration breaking continuous translation symmetry, will cause noncollinear spin configurations to arise.[32−36] Thus, a proper description of spin processes must come from a solution of the first-principles spin-dependent Hamiltonian that allows variational treatment of noncollinear spin. The generalized Hartree−Fock (GHF) method removes the spin-collinear constraint from conventional restricted and unrestricted Hartree−Fock (RHF and UHF) methods so that spins are allowed to rotate freely in a noncollinear framework. A detailed history of the early GHF method can be found in ref 37, and we refer readers to a recent review[36] on noncollinear spin. The GHF approach has been shown to be a convenient and inexpensive computational platform to simulate spin dynamics

Received: November 8, 2018
Published: November 28, 2018

DOI: 10.1021/acs.jctc.8b01140

of a single spin center in a static magnetic field[38] and in a dissociated reaction.[39]

In this work, we introduce a variational spin noncollinear approach using the complex GHF (ℂ-GHF) method with London orbitals in the presence of a strong magnetic field. The method implemented herein is able to model both spin-collinear and noncollinear phenomena as well as the processes underlying the magnetic field-induced spin phase transition. Note that during the preparation of this manuscript a variational GHF approach was applied to studies of orbital and spin effects in molecules subject to nonuniform magnetic fields.[40]

2. METHODOLOGY

2.1. Spinor Formalism of Generalized Hartree–Fock with London Orbitals. In order to treat noncollinear spins in a nonperturbative magnetic field, one needs to retain the full vector form of the magnetization $\mathbf{m}(\mathbf{r})$ and allow each spin quantization axis to rotate. This is equivalent to writing the spin orbitals as a superposition of the spin-up and spin-down manifolds. For Hartree–Fock, this leads to the GHF method,[32,34,36–38,41–43] which is similar in structure to the wave function used in two-component relativistic models.[44–53]

The spinor orbital is defined as

$$\psi_j(\mathbf{r}) = \begin{pmatrix} \phi_j^\alpha(\mathbf{r}) \\ \phi_j^\beta(\mathbf{r}) \end{pmatrix} \tag{1}$$

The spatial functions $\{\phi_j^\alpha(\mathbf{r},\mathbf{k}_\mathrm{A})\}$, $\{\phi_j^\beta(\mathbf{r},\mathbf{k}_\mathrm{A})\}$ are expanded in terms of a common set of complex London orbitals $\{\tilde{\chi}_\mu(\mathbf{r},\mathbf{k}_\mathrm{A})\}$

$$\phi_j^\alpha(\mathbf{r}, \mathbf{k}_\mathrm{A}) = \sum_\mu C_{\mu j}^\alpha \tilde{\chi}_\mu(\mathbf{r}, \mathbf{k}_\mathrm{A}) \tag{2}$$

$$\phi_j^\beta(\mathbf{r}, \mathbf{k}_\mathrm{A}) = \sum_\mu C_{\mu j}^\beta \tilde{\chi}_\mu(\mathbf{r}, \mathbf{k}_\mathrm{A}) \tag{3}$$

$$\tilde{\chi}_\mu(\mathbf{r}, \mathbf{k}_\mathrm{A}) = \chi_\mu(\mathbf{r} - \mathbf{R}_\mathrm{A}) e^{i\mathbf{k}_\mathrm{A}\cdot(\mathbf{r}-\mathbf{R}_\mathrm{A})} \tag{4}$$

where $\{\chi_\mu(\mathbf{r} - \mathbf{R}_\mathrm{A})\}$ are real AO basis functions centered at $\mathbf{R}_\mathrm{A}$. The exponential form of the London orbital phase factor defines the local gauge-origin at each nuclear center in the presence of a magnetic field with a plane wave vector described by $\mathbf{k}_\mathrm{A} = \frac{\mathbf{R}_\mathrm{A}\times\mathbf{B}}{2}$, where $\mathbf{B}$ is the external magnetic field.

In the spinor orbital basis defined in eq 1, the Fock matrix ($\mathbf{F}$) and the density matrix ($\mathbf{P}$ with $P_{\mu\nu}^{\sigma\sigma'} = \sum_j^{\mathrm{occ}} C_{\mu j}^\sigma C_{\nu j}^{\sigma'*}$) have a spin-blocked form,[38] shown in eq 5

$$\mathbf{X} = \begin{pmatrix} \mathbf{X}^{\alpha\alpha} & \mathbf{X}^{\alpha\beta} \\ \mathbf{X}^{\beta\alpha} & \mathbf{X}^{\beta\beta} \end{pmatrix} \qquad \mathbf{X} \in \{\mathbf{F}, \mathbf{P}\} \tag{5}$$

In the current implementation, we cast the rank-2 spin-blocked $\mathbf{F}$ and $\mathbf{P}$ matrices in the Pauli matrix basis[53]

$$\mathbf{F} = \sum_{n=0}^{3} \mathbf{F}_n \otimes \boldsymbol{\sigma}_n \tag{6}$$

$$\mathbf{P} = \sum_{n=0}^{3} \mathbf{P}_n \otimes \boldsymbol{\sigma}_n$$

$$\boldsymbol{\sigma}_0 = \begin{pmatrix} 1 & 0 \\ 0 & 1 \end{pmatrix} \quad \boldsymbol{\sigma}_1 = \begin{pmatrix} 0 & 1 \\ 1 & 0 \end{pmatrix} \quad \boldsymbol{\sigma}_2 = \begin{pmatrix} 0 & -i \\ i & 0 \end{pmatrix} \quad \boldsymbol{\sigma}_3 = \begin{pmatrix} 1 & 0 \\ 0 & -1 \end{pmatrix} \tag{7}$$

where the scalar ($\mathbf{F}_0$) and spin part ($\mathbf{F}_1$,$\mathbf{F}_2$,$\mathbf{F}_3$) of Fock matrix are defined as[53]

$$\mathbf{F}_0 = \mathbf{h}_0 + \mathbf{J}[\mathbf{P}_0] - \mathbf{K}[\mathbf{P}_0] \tag{8}$$

$$\mathbf{F}_n = \mathbf{h}_n - \mathbf{K}[\mathbf{P}_n] \qquad n = 1, 2, 3 \tag{9}$$

The Coulomb ($\mathbf{J}$) and exchange ($\mathbf{K}$) matrices are,

$$J_{\mu\nu}[\mathbf{P}_0] = \sum_{\lambda\kappa} (\mu\nu|\kappa\lambda) P_{0,\lambda\kappa} \tag{10}$$

$$K_{\mu\nu}[\mathbf{P}_n] = \sum_{\lambda\kappa} (\mu\lambda|\kappa\nu) P_{n,\lambda\kappa} \qquad n = 0, 1, 2, 3 \tag{11}$$

where

$$(\mu\nu|\kappa\lambda) = \int d^3\mathbf{r}_1 \int d^3\mathbf{r}_2 \frac{\tilde{\chi}_\mu^*(\mathbf{r}_1, \mathbf{k}_\mathrm{A})\tilde{\chi}_\nu(\mathbf{r}_1, \mathbf{k}_\mathrm{B})\tilde{\chi}_\kappa^*(\mathbf{r}_2, \mathbf{k}_\mathrm{C})\tilde{\chi}_\lambda(\mathbf{r}_2, \mathbf{k}_\mathrm{D})}{|\mathbf{r}_1 - \mathbf{r}_2|} \tag{12}$$

are the electron repulsion integrals (ERIs). Note that because ERIs using London orbitals are complex valued they only have a four-fold symmetry instead of eight, as in the case of real-valued ERIs

$$(\mu\nu|\kappa\lambda) = (\kappa\lambda|\mu\nu) = (\nu\mu|\lambda\kappa)^* = (\lambda\kappa|\nu\mu)^* \tag{13}$$

2.2. Nonrelativistic Hamiltonian in the Presence of a Static and Uniform Magnetic Field. In the nonrelativistic framework, the interaction of an electron spin with external electromagnetic field is described by the Schrödinger-Pauli Hamiltonian:

$$\hat{h}^{\mathrm{Pauli}} = \frac{1}{2}[\boldsymbol{\sigma}\cdot(\mathbf{p} + \mathbf{A})]^2 - \hat{U} \tag{14}$$

where $\mathbf{A}$ and $\hat{U}$ are the vector potential and scalar potential of the electromagnetic field, respectively. $\mathbf{p} = -i\nabla$ is the momentum operator. Given the relationship between the vector potential and the magnetic field, $\mathbf{A} = \frac{1}{2}\mathbf{B} \times \mathbf{r}$, the one-electron Pauli Hamiltonian can be written as

$$h^{\mathrm{Pauli}} = \hat{h}_0(\mathbf{r}) + \frac{1}{2}(\boldsymbol{\sigma} - i\mathbf{r} \times \nabla)\cdot\mathbf{B} + \frac{1}{8}(\mathbf{B} \times \mathbf{r})^2 \tag{15}$$

where $\hat{h}_0(\mathbf{r})$ is the field-free one-electron Hamiltonian. The second term includes spin and orbital Zeeman contributions. The third term is the diamagnetic contribution and is quadratic in the strength of the magnetic field, which can be expanded as

$$\begin{aligned}(\mathbf{B} \times \mathbf{r})^2 = {} & ({B_y}^2 + {B_z}^2)x^2 + ({B_x}^2 + {B_z}^2)y^2 \\ & + ({B_x}^2 + {B_y}^2)z^2 - 2B_xB_yxy - 2B_yB_zyz - 2B_xB_zxz\end{aligned} \tag{16}$$

The orbital Zeeman and the diamagnetic term do not directly contribute to the spin dynamics.[38] Although these two terms are relatively small, they are important contributions in diamagnetism.[54–57] In the presence of a strong magnetic field, these two terms account for significant contributions to the interaction between the chemical system and the external field.[26]

Using the formalism of generalized Hartree–Fock in the Pauli matrix basis (eq 6), spin contributions in eq 14 can be separated from the scalar part. The resulting scalar Fock matrix is

DOI: 10.1021/acs.jctc.8b01140
J. Chem. Theory Comput. 2019, 15, 348–356

$$\mathbf{F}_0 = \mathbf{h}_0 + \mathbf{J}[\mathbf{P}_0] - \mathbf{K}[\mathbf{P}_0] - \frac{\mathrm{i}}{2}\mathbf{L}\cdot\mathbf{B} + \frac{1}{8}\{(B_y{}^2 + B_z{}^2)\mathbf{q}_{xx} + (B_x{}^2 + B_z{}^2)\mathbf{q}_{yy} + (B_x{}^2 + B_y{}^2)\mathbf{q}_{zz} - 2B_xB_y\mathbf{q}_{xy} - 2B_yB_z\mathbf{q}_{yz} - 2B_xB_z\mathbf{q}_{xz}\} \quad (17)$$

where $\mathbf{L}_{\mu\nu} = \langle\tilde{\chi}_\mu|\mathbf{r} \times \nabla|\tilde{\chi}_\nu\rangle$ is the orbital-angular momentum integral and $(\mathbf{q}_{nm})_{\mu\nu} = \langle\tilde{\chi}_\mu|\hat{r}_n\hat{r}_m|\tilde{\chi}_\nu\rangle$ is the electric quadrupole integral. After spin separation using the Pauli matrices, spin components of the Fock matrix are

$$\mathbf{F}_n = \frac{1}{2}B_n\mathbf{S} - \mathbf{K}[\mathbf{P}_n] \qquad n = 1, 2, 3 \quad (18)$$

where **S** is the overlap matrix.

2.3. Electron Integrals Using London-Type Orbitals.

The electronic structure method introduced in this work requires the computation of one- and two-electron integrals of London orbitals. Integrals are evaluated in complex arithmetic, and the corresponding recursion relationships are presented in the Appendix. In the current work, one- and two-electron integrals of London orbitals and the complex generalized Hartree−Fock method are implemented in the Chronus Quantum software package.[58]

3. RESULTS AND DISCUSSION

The formalism of GHF in the spinor basis allows for calculations of noncollinear spin states within the ab initio framework. With the atomic London orbitals and associated one- and two-electron integrals, wave functions of chemical systems with multispin centers in the presence of a static magnetic field can be variationally optimized. In this current work, we study the spin noncollinearity and magnetic phase transition of molecular systems driven by static magnetic fields. All ℂ-GHF calculations are done using the Chronus Quantum software package.

The first test case is a H_2 molecule in a uniform magnetic field. ℂ-GHF solutions in the presence of a static magnetic field were obtained with several different basis sets, including 6-31G, 6-31G(d,p), aug-cc-pVDZ, and aug-cc-pVTZ. Although differences in the absolute energy computed with different basis sets are noticeable, the expectation values of S_z at a given magnetic field only differ by less than 3%. In the following discussion, we will only present the results computed at the ℂ-GHF/aug-cc-pVTZ level of theory.[59] In this test system, the static magnetic field (1 au ≈ 2.35×10^5 T, based on SI units for the magnetic field) is aligned perpendicular to the molecular bond axis. Figure 1 plots the potential energy curve of a H_2 molecule in a uniform magnetic field ($|B_z| = 0.001$ au along the $-z$ direction) computed using the complex generalized Hartree−Fock (ℂ-GHF), complex unrestricted Hartree−Fock (ℂ-UHF), and complex restricted Hartree−Fock (ℂ-RHF) with London orbitals. ℂ-UHF and ℂ-RHF calculations are restricted to spin triplet ($S_z = 1$) and singlet ($S_z = 0$) states, respectively. The ℂ-GHF solution is not spin-restricted. As a result, at all bond distances, the ℂ-GHF solution is always the lowest in energy.

From the equilibrium bond length toward the asymptotic dissociation limit, the change in $\langle S_z\rangle$ of the ℂ-GHF solution suggests that the system undergoes a spin phase transition from $\langle S_z\rangle = 0$ to 1. This spin phase transition is a result of the competing driving forces of the exchange coupling and paramagnetism. This can be understood from the perturbative and phenomenological spin Hamiltonian including both the spin exchange coupling and Zeeman effect

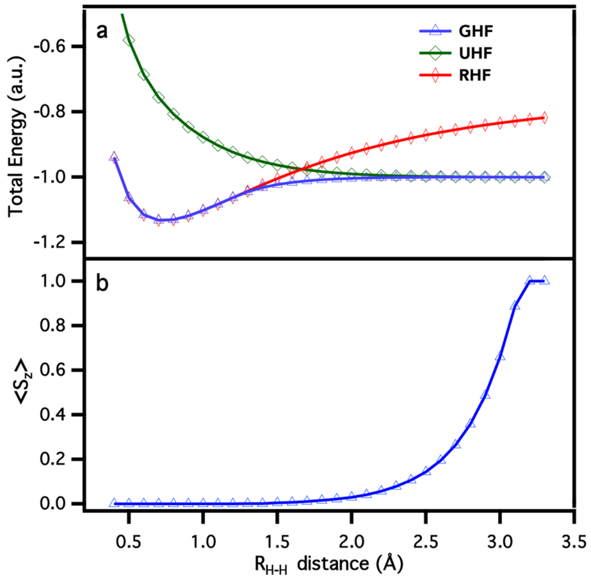

Figure 1. (a) Potential energy surface of a H_2 molecule in a homogeneous magnetic field, $|B_z| = 0.001$ au along the $-z$ direction. (b) Expectation value of S_z for the ℂ-GHF solution.

$$H = -\frac{1}{2}J_{12}\mathbf{S}_1\cdot\mathbf{S}_2 - g\mu_{\mathrm{B}}\mathbf{B}\cdot(\mathbf{S}_1 + \mathbf{S}_2) \quad (19)$$

$$= -\frac{1}{2}J_{12}|\mathbf{S}_1||\mathbf{S}_2|\cos(\theta) - g\mu_{\mathrm{B}}B_z(S_{1z} + S_{2z}) \quad (20)$$

where J_{12} is the exchange coupling strength, g is the spin g-factor, and μ_{B} is the Bohr magneton. For noncollinear spin alignment in the presence of a static magnetic field in the z direction depicted in Figure 2, the spin Hamiltonian can be written as in eq 20, with the angle between the two spin vectors defined as θ. In the collinear spin electronic structure framework, such as RHF and UHF, θ can only be 0 or 180°. Without spin−orbit coupling, the exchange coupling is isotropic.

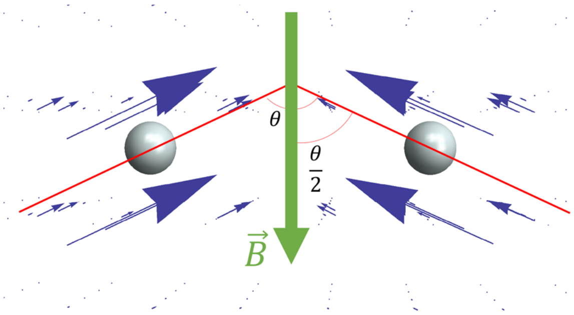

Figure 2. Illustration of noncollinearity of two spin vectors.

At the equilibrium bond distance, the exchange coupling is much stronger than the Zeeman term, giving rise to the antiparallel orientation of the two electrons, i.e., a closed-shell configuration and $\theta = 180°$. As the bond length increases, the exchange coupling decreases exponentially, whereas the strength of the Zeeman effect remains constant. At certain bond lengths when the exchange coupling becomes weaker than the Zeeman term, the electronic system undergoes a spin phase transition. This spin phase transition is a noncollinear process where θ can take on any value between 0 and 180°, and the noncollinear spin state has the lowest energy. In this regime, only the noncollinear $\mathbb{C}$-GHF can describe the electronic characteristics of the spin system.

Figure 3 shows the progression of spin vectors during the spin phase transition when the bond length is stretched from 2.6 to 3.1 Å while keeping the magnetic field strength constant, $|B_z| = 0.001$ au, along the $-z$ direction. When a nonzero $\langle S_z \rangle$ moment is obtained in the system, the overall spin vector is aligned opposite to the magnetic field arising from the spin Zeeman effect. As the spins undergo a phase transition, the angle between local spin vectors decreases from 180 to 0°. At $R_{\mathrm{HH}} \approx 2.9$ Å (Figure 3b), the two local spin vectors are nearly orthogonal, exhibiting a strong noncollinearity in the presence of a magnetic field. The UHF and RHF solutions are restricted by collinear spin configuration and, therefore, cannot capture the progression of spin phase transition via the spin noncollinear configuration.

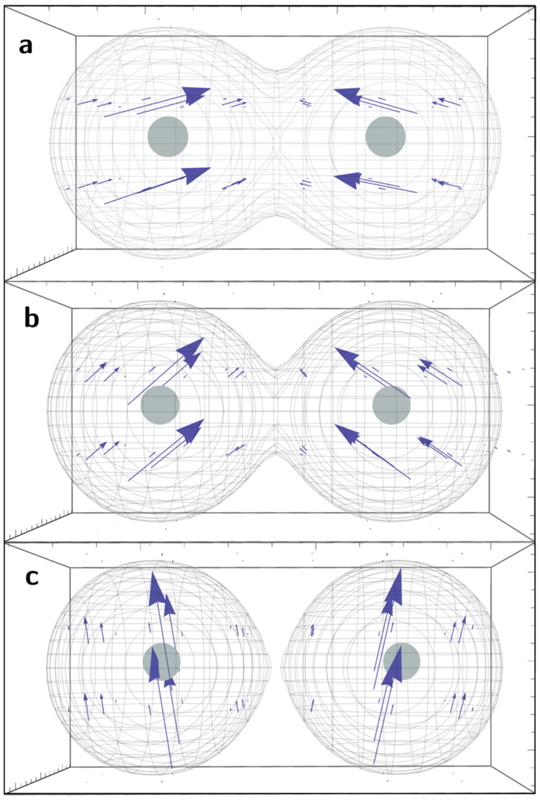

Figure 3. Spin magnetization vectors at different H−H bond lengths. (a) $R_{\mathrm{HH}} = 2.6$ Å, $\langle S_z \rangle = 0.19428$, (b) $R_{\mathrm{HH}} = 2.9$ Å, $\langle S_z \rangle = 0.48588$, and (c) $R_{\mathrm{HH}} = 3.1$ Å, $\langle S_z \rangle = 0.88685$. For all cases, the magnetic field strength is 0.001 au along the $-z$ direction. The area enclosed by the mesh has a charge density of >0.002. The size of the 3D box is 550 pm(W) × 300 pm(H) × 300 pm(D).

The framework of $\mathbb{C}$-GHF with London orbitals also allows for a variational exploration of critical magnetic field strengths that can induce a spin phase transition in molecular systems. Figure 4 plots the spin magnetization vectors at different field strengths while keeping the bond length fixed at 2.6 Å. As the magnetic field gets stronger, the expectation value of S_z becomes greater, and a noncollinear spin phase transition is observed. In contrast to the phenomenon in Figure 3 where bond stretching weakens the exchange coupling, the spin phase transition in Figure 4 arises from the increasing strength of the spin Zeeman effect due to the increase in magnetic field strength. At $|B_z| = 0.005$ au, the spin phase transition is already complete, and the triplet spin-collinear configuration is the lowest-energy state.

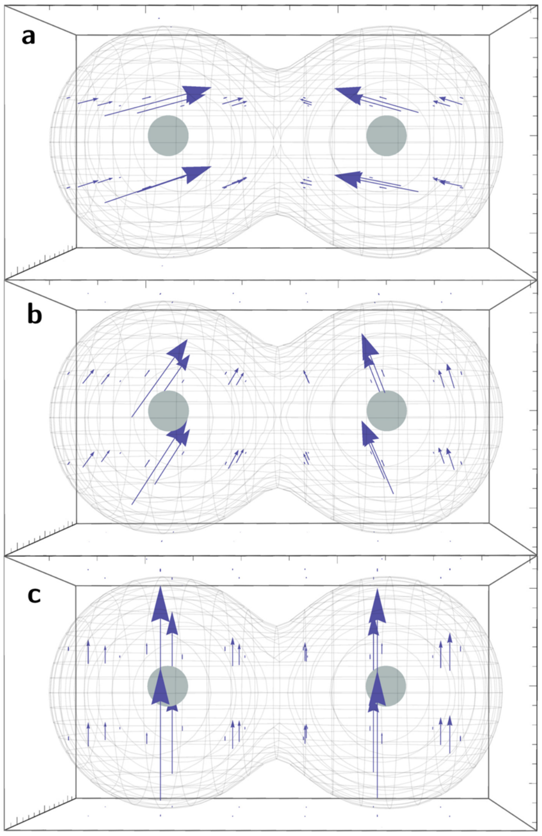

Figure 4. Spin magnetization vectors for H_2 at different field strengths. (a) $|B_z| = 0.001$ au, $\langle S_z \rangle = 0.19428$, (b) $|B_z| = 0.003$ au, $\langle S_z \rangle = 0.59040$, and (c) $|B_z| = 0.005$ au, $\langle S_z \rangle = 1.0000$. The H−H bond length is $R_{\mathrm{HH}} = 2.6$ Å. The area enclosed by the mesh has a charge density of >0.002. The size of the 3D box is 550 pm(W) × 300 pm(H) × 300 pm(D).

Figure 5 plots the expectation value of S_z as a function of H−H bond length and magnetic field strength. Figure 5 suggests that the rate of the spin phase transition sensitively depends on the strength of exchange coupling and spin Zeeman terms. At near the equilibrium bond distance with the strongest magnetic field ($|B_z| = 0.3$ au) considered here, the spin configuration switches almost immediately. In the weak field or weak exchange coupling regime, spins can be seen to undergo a much slower phase transition compared to those in the strong field or strong exchange coupling regime.

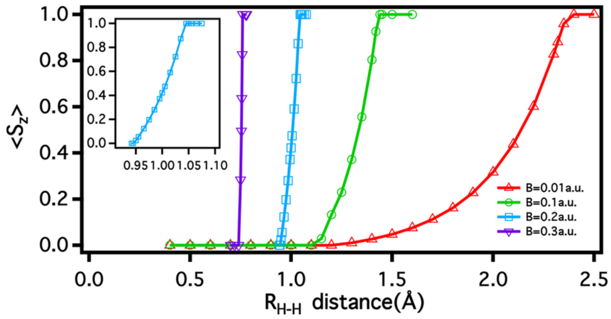

Figure 5. $\langle S_z \rangle$ as a function of H−H bond length and magnetic field strength.

DOI: 10.1021/acs.jctc.8b01140
J. Chem. Theory Comput. 2019, 15, 348−356

Although the orbital Zeeman and diamagnetic terms in eq 15 do not directly modify the spin interaction with the external magnetic field, they are important contributions to the stability of the molecular system in a magnetic field and can indirectly influence spin dynamics through perturbation of the spatial extent and energetics of molecular orbitals.[28] Figure 6 shows the magnitudes of spin Zeeman, orbital Zeeman, and diamagnetic contributions to the total potential energy. In the strong exchange couple regime ($R_{HH} \approx 0.4{-}0.6$ Å), the diamagnetic term has the largest contribution, followed by the orbital Zeeman term. These two terms are different in sign, with the diamagnetic term destabilizing the system energy with respect to the field-free molecular system. In this regime, the system takes on a closed-shell configuration. As a result, the spin Zeeman contribution is zero. As the system undergoes a spin phase transition, the nonzero overall spin vector gives rise to an increasing spin Zeeman contribution that significantly stabilizes the molecular system. Analysis of Figure 6 suggests that in a closed-shell configuration orbital Zeeman and diamagnetic contributions are responsible for the interaction between the electronic system and the external magnetic field. In an open-shell system, the spin Zeeman is the dominant driving force underlying the system−magnetic field interaction in the weak field regime. As the field strength increases, the diamagnetic term becomes non-negligible as it increases quadratically with respect to the field.

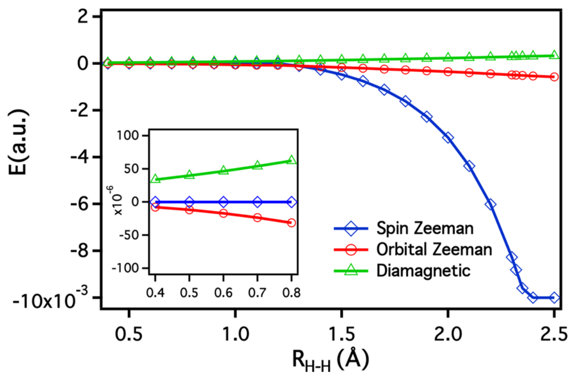

Figure 6. Energetic contributions of spin Zeeman, orbital Zeeman, and diamagnetic terms. $|B_z| = 0.01$ au.

In order to probe the spin phase transition in a more complex magnetic molecular system, we study the spin characteristics of a dichromium molecular complex, $[(H_3N)_4Cr(OH)_2Cr(NH_3)_4]^{4+}$, in a uniform magnetic field. Figure 7 illustrates the molecular structure and computational setup where the magnetic field is applied in the $+z$ direction, perpendicular to the Cr−O−Cr−O plane. The molecular geometry was optimized[60] with the GAUSSIAN16 software package[61] at the B3LYP/6-31G level of theory.[62−65] The electronic structures in a magnetic field were calculated using ℂ-GHF with 6-31G London AOs in the Chronus Quantum software package.

In the di-Cr(III) molecular complex, the octahedral ligand field splits Cr d orbitals into e and t_2 sets, where three unpaired electrons occupy the t_2 manifold (Figure 8b). In contrast to the previous molecular H_2 system where the ground state at equilibrium bond length is in a nonmagnetic closed-shell configuration, the ground state of the di-Cr(III) molecular complex exhibits a magnetic ℂ-GHF solution. Cr(III) cations in an octahedral coordination environment bridged by oxygen atoms are known to have antiferromagnetic superexchange coupling.[66−68] The J constant in eq 20 for superexchange coupling is negative in sign, favoring the antiferromagnetic spin alignment in the ground state ($\langle S_z \rangle = 0$; see Figure 8b). The lack of electron correlation in Hartree−Fock calculation gives rise to an overestimation of the J constant magnitude because the correlation effect has an opposite contribution to the magnetism.[66] Nevertheless, qualitative characteristics and trends of spin phase transitions can still be captured by ℂ-GHF calculations with London AOs.

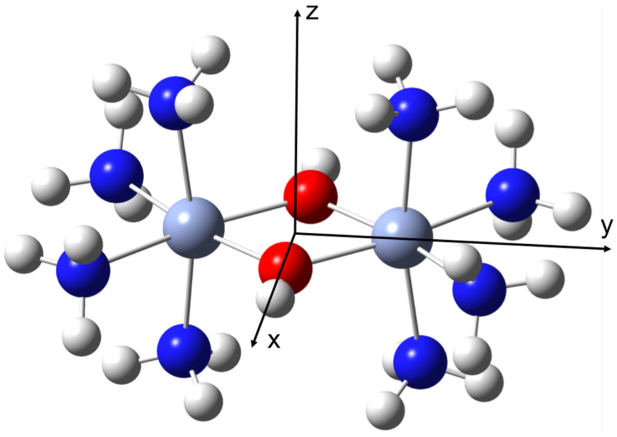

Figure 7. Molecular structure of a dichromium molecular complex, $[(H_3N)_4Cr(OH)_2Cr(NH_3)_4]^{4+}$ that has D_{2h} symmetry. Each Cr atom is in a distorted octahedral coordination environment. The magnetic field is applied in the $+z$ direction, perpendicular to the Cr−O−Cr−O plane.

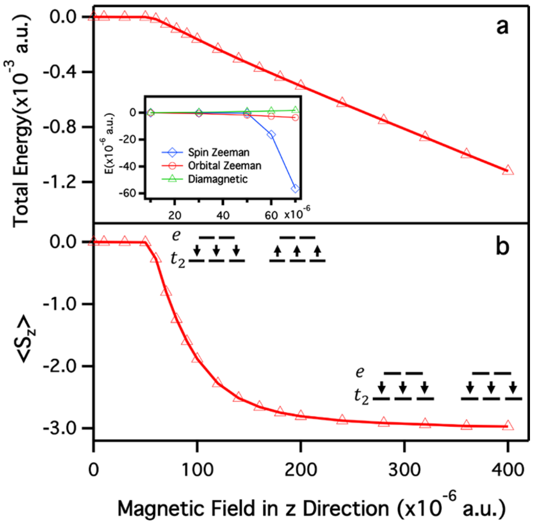

Figure 8. (a) Total energy of the di-Cr(III) complex in a finite magnetic field. (b) Expectation value of S_z of the ℂ-GHF solution.

In the absence of an external magnetic field, the ground-state wave function of the di-Cr(III) molecular complex obtained from the ℂ-GHF calculation is antiferromagnetic. Figure 8 plots the relative total energy compared to that in the absence of a magnetic field and the expectation value of S_z as a function of applied magnetic field strength. When the magnetic field is relatively weak, the system is in the antiferromagnetic state. In this region, the superexchange coupling is constant and the small energy change is solely due to the orbital Zeeman and diamagnetic terms. As the magnetic field reaches a critical point ($\sim 60 \times 10^{-6}$ au) where a small change in spin alignment can give rise to a spin Zeeman term strong enough to overcome the antiferromagnetic superexchange coupling, the system starts to undergo a spin phase transition. As the magnetic field strength increases, the energy of the molecule decreases due to the increasing spin Zeeman contribution. The change of expectation value of S_z indicates that the spin state gradually switches from the antiferromagnetic $\langle S_z\rangle = 0$ to ferromagnetic $\langle S_z\rangle = -3$ configuration (Figure 8b). This case study suggests that ℂ-GHF calculations with London AOs can be used to investigate magnetic phase transitions in transition metal complexes.

4. CONCLUSIONS

Presented in this article is a framework of an ab initio variational approach using complex generalized Hartree–Fock (ℂ-GHF) with London orbitals to effectively explore the spin phase space in the presence of a homogeneous magnetic field. We introduced the implementation of the ℂ-GHF approach within the spinor formalism. In order to account for gauge-origin independence in the self-consistent field, the ℂ-GHF is represented in the London orbital basis with a magnetic field complex phase factor. Recursive algorithms for computing one- and two-electron integrals of London orbitals are provided in the Appendix. Additionally, a Pauli matrix representation of the ℂ-GHF is introduced in this work that allows for the separation of spin contributions from the scalar part of the Fock matrix.

ℂ-GHF with London orbitals in the presence of a homogeneous magnetic field has been applied to study the spin phase transition in a molecular H_2 system. Noncollinear spin configurations have been observed during the phase transition from a singlet to triplet state. The competing driving forces of exchange coupling and the spin Zeeman effect have been shown to govern the spin phase transition and its transition rate. In addition, energetic analysis suggests that in the presence of a static magnetic field orbital Zeeman and diamagnetic terms are important contributions in a closed-shell configuration, while the spin Zeeman term is the dominant interaction driving force in an open-shell state.

The variational ℂ-GHF method with London orbitals can also be used to compute magnetic phase transitions in molecular complexes driven by an external magnetic field. Results show that there exists a critical point where the spin Zeeman is large enough to compete with the superexchange coupling so that the spin phase transition takes place and drives the magnetic phase transition.

The method presented in this work is based on the single Slater determinant wave function ansatz, which lacks important electron correlation effects. Future developments will use the variational ℂ-GHF reference for correlated electronic structure methods, which will provide more accurate descriptions of spin and magnetic phase transitions.

■ APPENDIX. INTEGRAL EVALUATION

A London orbital is defined as

$$\tilde{\chi}(\mathbf{r}, \mathbf{k}_A) = \chi(\mathbf{r} - \mathbf{R}_A)e^{i\mathbf{k}_A\cdot(\mathbf{r}-\mathbf{R}_A)} \tag{21}$$

where $\{\chi\}$ are primary atom-centered Gaussian-type orbitals

$$\chi_a = (x - A_x)^{a_x}(y - A_y)^{a_y}(z - A_z)^{a_z}e^{-\zeta_a|\mathbf{r}-\mathbf{A}|} \tag{22}$$

$$|\mathbf{r} - \mathbf{A}| = \sqrt{(x - A_x)^2 + (y - A_y)^2 + (z - A_z)^2} \tag{23}$$

$\mathbf{A} = \{A_x, A_y, A_z\}$ is the coordinate of the atom center and $\mathbf{a} = \{a_x, a_y, a_z\}$ is the angular momentum. ζ_a is the exponent of primary Gaussian-type orbitals.

The London orbital defined in eq 21 has the following identity

$$\tilde{\chi}_\mu^*(\mathbf{r}, \mathbf{k}_A) = \tilde{\chi}_\mu(\mathbf{r}, -\mathbf{k}_A) \tag{24}$$

The one-electron integral for any one-electron operator $\hat{O}_1$ can be defined as

$$\begin{aligned}(\mathbf{a}|\hat{O}_1|\mathbf{b}) &= \int d^3\mathbf{r}\, \tilde{\chi}^*(\mathbf{r}, \mathbf{k}_A)\hat{O}_1\tilde{\chi}(\mathbf{r}, \mathbf{k}_B)\\ &= \int d^3\mathbf{r}\, \tilde{\chi}(\mathbf{r}, -\mathbf{k}_A)\hat{O}_1\tilde{\chi}(\mathbf{r}, \mathbf{k}_B)\end{aligned} \tag{25}$$

and for a two-electron operator $\hat{O}_2$, the integral is defined as

$$\begin{aligned}(\mathbf{ab}|\hat{O}_2|\mathbf{cd}) &= \int d^3\mathbf{r}_1 \int d^3\mathbf{r}_2\, \tilde{\chi}^*(\mathbf{r}_1, \mathbf{k}_A)\tilde{\chi}(\mathbf{r}_1, \mathbf{k}_B)\hat{O}_2\tilde{\chi}^*(\mathbf{r}_2, \mathbf{k}_C)\tilde{\chi}(\mathbf{r}_2, \mathbf{k}_D)\\ &= \int d^3\mathbf{r}_1 \int d^3\mathbf{r}_2\, \tilde{\chi}(\mathbf{r}_1, -\mathbf{k}_A)\tilde{\chi}(\mathbf{r}_1, \mathbf{k}_B)\hat{O}_2\tilde{\chi}(\mathbf{r}_2, -\mathbf{k}_C)\tilde{\chi}(\mathbf{r}_2, \mathbf{k}_D)\end{aligned} \tag{26}$$

General recursion relationships for one- and two-electron integrals using mixed plane-wave/Gaussian-type orbitals were presented by Obara and co-workers,[69] and the application to London orbitals was developed by Helgaker and Teale.[25,70] In this work, we use a modified Obara–Saika algorithm to calculate one- and two-electron integrals using London orbitals. As the derivations are similar to those in references,[69,25] we only present the working equations used in this work without going through the detailed mathematics. Note that recursive algorithms presented herein can be used for evaluating integrals of mixed plane-wave/Gaussian orbitals with an arbitrary wave vector.

The following intermediate quantities are defined for integral recursion relationships used in this work

$$\zeta = \zeta_a + \zeta_b \tag{27}$$

$$\eta = \zeta_c + \zeta_d \tag{28}$$

$$\xi = \frac{\zeta_a\zeta_b}{\zeta_a + \zeta_b} \tag{29}$$

$$\rho = \frac{\zeta\eta}{\zeta + \eta} \tag{30}$$

$$\mathbf{P} = \frac{\zeta_a A + \zeta_b B}{\zeta_a + \zeta_b} \tag{31}$$

$$\mathbf{Q} = \frac{\zeta_c C + \zeta_d D}{\zeta_c + \zeta_d} \tag{32}$$

$$\mathbf{W} = \frac{\zeta P + \eta Q}{\zeta + \eta} \tag{33}$$

$$\mathbf{k}_p = -\mathbf{k}_a + \mathbf{k}_b \tag{34}$$

$$\mathbf{k}_q = -\mathbf{k}_c + \mathbf{k}_d \tag{35}$$

A.1. Overlap Integral

The recursion for the overlap integral is

$$(\mathbf{a} + \mathbf{1}_\mu \| \mathbf{b}) = \left(\mathbf{P} + \frac{\mathrm{i}(-\mathbf{k}_\mathrm{a} + \mathbf{k}_\mathrm{b})}{2\zeta} - \mathbf{A}\right)_\mu (\mathbf{a}\|\mathbf{b}) + \frac{1}{2\zeta}\{N_\mu(\mathbf{a})(\mathbf{a} - \mathbf{1}_\mu\|\mathbf{b}) + N_\mu(\mathbf{b})(\mathbf{a}\|\mathbf{b} - \mathbf{1}_\mu)\} \tag{36}$$

$$(\mathbf{0}_\mathrm{A}\|\mathbf{0}_\mathrm{B}) = \left(\frac{\pi}{\zeta}\right)^{3/2} \mathrm{e}^{-\xi(\mathbf{A}-\mathbf{B})^2} \mathrm{e}^{-(-\mathbf{k}_\mathrm{a}+\mathbf{k}_\mathrm{b})^2/4\zeta} \mathrm{e}^{\mathrm{i}\{(-\mathbf{k}_\mathrm{a})\cdot(\mathbf{P}-\mathbf{A})+\mathbf{k}_\mathrm{b}\cdot(\mathbf{P}-\mathbf{B})\}} \tag{37}$$

where $N_\mu(\mathbf{a})$ is the μ component of the angular momentum $\mathbf{a}$. $\mathbf{a} \pm \mathbf{1}_\mu$ means that the μ component of the angular momentum $\mathbf{a}$ is raised/lowered by 1.

A.2. Kinetic Energy Integral

The kinetic integral is the second derivative of the overlap integral

$$(\mathbf{a}|\mathcal{T}|\mathbf{b}) = -\frac{1}{2}\sum_{\nu=x,y,z}(\mathbf{a}\|\partial_\nu{}^2\mathbf{b}) \tag{38}$$

The recursion relationship for the kinetic energy integral is

$$-\frac{1}{2}(\mathbf{a}\|\partial_\nu{}^2\mathbf{b}) = -2\zeta_\mathrm{b}{}^2(\mathbf{a}\|\mathbf{b} + \mathbf{2}_\nu) + 2\mathrm{i}\zeta_\mathrm{b}k_{\mathrm{b}\mu}(\mathbf{a}\|\mathbf{b} + \mathbf{1}_\nu) + \left(2\zeta_\mathrm{b}N_\nu(\mathbf{b}) + \zeta_\mathrm{b} + \frac{1}{2}\mathbf{k}_{\mathrm{b}\nu}{}^2\right)(\mathbf{a}\|\mathbf{b}) - \mathrm{i}N_\nu(\mathbf{b})k_{\mathrm{b}\nu}(\mathbf{a}\|\mathbf{b} - \mathbf{1}_\nu) - \frac{1}{2}N_\nu(\mathbf{b})(N_\nu(\mathbf{b}) - 1)(\mathbf{a}\|\mathbf{b} - \mathbf{2}_\nu) \tag{39}$$

where $k_{\mathrm{b}\mu}$ is the μ component of the wave vector $\mathbf{k}_\mathrm{b}$.

A.3. Angular Momentum Integral

The angular momentum integral is defined as

$$\begin{aligned}(\mathbf{a}|\mathbf{r} \times \nabla|\mathbf{b}) &= \hat{\mathbf{x}}(\mathbf{a}|r_y\partial_z - r_z\partial_y|\mathbf{b}) + \hat{\mathbf{y}}(\mathbf{a}|r_z\partial_x - r_x\partial_z|\mathbf{b}) + \hat{\mathbf{z}}(\mathbf{a}|r_x\partial_y - r_y\partial_x|\mathbf{b}) \\ &= -\hat{\mathbf{x}}(\mathbf{a}|r_y\partial_{B_z} - r_z\partial_{B_y}|\mathbf{b}) - \hat{\mathbf{y}}(\mathbf{a}|r_z\partial_{B_x} - r_x\partial_{B_z}|\mathbf{b}) - \hat{\mathbf{z}}(\mathbf{a}|r_x\partial_{B_y} - r_y\partial_{B_x}|\mathbf{b})\end{aligned} \tag{40}$$

where $\hat{\mathbf{x}}$, $\hat{\mathbf{y}}$, and $\hat{\mathbf{z}}$ are unit vectors in the x, y, and z directions. ∂_{B_μ} is the partial derivative with respect to nuclear coordinates at atom center B. The integral of the type $(\mathbf{a}|r_\mu\partial_\nu|\mathbf{b})$ where $\mu,\nu = x,y,z$ can be evaluated as linear combinations of overlap integrals

$$(\mathbf{a}|r_\mu\partial_\nu|\mathbf{b}) = -\{2\zeta_\mathrm{b}(\mathbf{a} + \mathbf{1}_\mu\|\mathbf{b} + \mathbf{1}_\nu) - N_\nu(\mathbf{b})(\mathbf{a} + \mathbf{1}_\mu\|\mathbf{b} - \mathbf{1}_\nu) - \mathrm{i}k_{\mathrm{b}\nu}(\mathbf{a} + \mathbf{1}_\mu\|\mathbf{b})\} - A_\mu\{2\zeta_\mathrm{b}(\mathbf{a}\|\mathbf{b} + \mathbf{1}_\nu) - N_\nu(\mathbf{b})(\mathbf{a}\|\mathbf{b} - \mathbf{1}_\nu) - \mathrm{i}k_{\mathrm{b}\nu}(\mathbf{a}\|\mathbf{b})\} \tag{41}$$

A.4. Electric Quadrupole Integral

The recursion relationship for the electric quadrupole integral is

$$(\mathbf{a}|r_\mu r_\nu|\mathbf{b}) = (\mathbf{a} + \mathbf{1}_\mu\|\mathbf{b} + \mathbf{1}_\nu) + A_\mu(\mathbf{a}\|\mathbf{b} + \mathbf{1}_\nu) + B_\nu(\mathbf{a} + \mathbf{1}_\mu\|\mathbf{b}) + A_\mu B_\nu(\mathbf{a}\|\mathbf{b}) \tag{42}$$

A.5. Nuclear Attraction Integral

Define the operator

$$V = \frac{1}{|\mathbf{r} - \mathbf{C}|} \tag{43}$$

where $\mathbf{C}$ is the nuclear coordinate. The recursion for nuclear attraction integral is

$$\begin{aligned}(\mathbf{a} + \mathbf{1}_\mu|V|\mathbf{b})^{(m)} &= \left(\mathbf{P} + \frac{\mathrm{i}\mathbf{k}_{\mathrm{p}\mu}}{2\zeta} - \mathbf{A}\right)_\mu (\mathbf{a}|V|\mathbf{b})^{(m)} - \left(\mathbf{P} + \frac{\mathrm{i}\mathbf{k}_{\mathrm{p}\mu}}{2\zeta} - \mathbf{C}\right)_\mu (\mathbf{a}|V|\mathbf{b})^{(m+1)} \\ &+ \frac{1}{2\zeta}N_\mu(\mathbf{a})\{(\mathbf{a} - \mathbf{1}_\mu|V|\mathbf{b})^{(m)} - (\mathbf{a} - \mathbf{1}_\mu|V|\mathbf{b})^{(m+1)}\} \\ &+ \frac{1}{2\zeta}N_\mu(\mathbf{b})\{(\mathbf{a}|V|\mathbf{b} - \mathbf{1}_\mu)^{(m)} - (\mathbf{a}|V|\mathbf{b} - \mathbf{1}_\mu)^{(m+1)}\}\end{aligned} \tag{44}$$

$$(\mathbf{0}_\mathrm{A}|V|\mathbf{0}_\mathrm{B})^{(m)} = 2\left(\frac{\zeta}{\pi}\right)^{1/2}(\mathbf{0}_\mathrm{A}\|\mathbf{0}_\mathrm{B})F_\mathrm{m}(T) \tag{45}$$

$$T = \zeta\left(\mathbf{P} - \mathbf{C} + \mathrm{i}\frac{-\mathbf{k}_\mathrm{a} + \mathbf{k}_\mathrm{b}}{2\zeta}\right)^2 \tag{46}$$

where $F_\mathrm{m}(T)$ is Boys function.

A.6. Electron Repulsion Integral

The recursion for ERI is

$$\begin{aligned}((\mathbf{a} + \mathbf{1}_\mu)\mathbf{b}|\mathbf{cd})^{(m)} &= \left(\mathbf{P} - \mathbf{A} + \frac{\mathrm{i}\mathbf{k}_{\mathrm{p}\mu}}{2\zeta}\right)_\mu (\mathbf{ab}|\mathbf{cd})^{(m)} + \left(\mathbf{W} - \mathbf{P} - \frac{\mathrm{i}\rho(-\mathbf{k}_\mathrm{a} + \mathbf{k}_\mathrm{b})_\mu}{2\zeta^2} + \frac{\mathrm{i}(-\mathbf{k}_\mathrm{c} + \mathbf{k}_\mathrm{d})_\mu}{2(\zeta + \eta)}\right)_\mu (\mathbf{ab}|\mathbf{cd})^{(m+1)} \\ &+ \frac{1}{2\zeta}N_\mu(\mathbf{a})\left\{((\mathbf{a} - \mathbf{1}_\mu)\mathbf{b}|\mathbf{cd})^{(m)} - \frac{\rho}{\zeta}((\mathbf{a} - \mathbf{1}_\mu)\mathbf{b}|\mathbf{cd})^{(m+1)}\right\} + \frac{1}{2\zeta}N_\mu(\mathbf{b})\left\{(\mathbf{a}(\mathbf{b} - \mathbf{1}_\mu)|\mathbf{cd})^{(m)} - \frac{\rho}{\zeta}(\mathbf{a}(\mathbf{b} - \mathbf{1}_\mu)|\mathbf{cd})^{(m+1)}\right\} \\ &+ \frac{1}{2(\zeta + \eta)}\{N_\mu(\mathbf{c})(\mathbf{ab}|(\mathbf{c} - \mathbf{1}_\mu)\mathbf{d})^{(m+1)} + N_\mu(\mathbf{d})(\mathbf{ab}|\mathbf{c}(\mathbf{d} - \mathbf{1}_\mu))^{(m+1)}\}\end{aligned} \tag{47}$$

$$(\mathbf{00}|\mathbf{00})^{(m)} = 2\left(\frac{\rho}{\pi}\right)^{1/2}(\mathbf{0}_\mathrm{A}\|\mathbf{0}_\mathrm{B})(\mathbf{0}_\mathrm{C}\|\mathbf{0}_\mathrm{D})F_\mathrm{m}(T) \tag{48}$$

$$T = \rho\left[\left(\mathbf{P} + \mathrm{i}\frac{\mathbf{k}_\mathrm{p}}{2\zeta}\right) - \left(\mathbf{Q} + \mathrm{i}\frac{\mathbf{k}_\mathrm{q}}{2\eta}\right)\right]^2 \tag{49}$$

where F_m is the Boys function. The horizontal recursion can be derived from eq 47 easily.[71]

$$(\mathbf{a}(\mathbf{b} + \mathbf{1}_\mu)|\mathbf{cd})^{(m)} = ((\mathbf{a} + \mathbf{1}_\mu)\mathbf{b}|\mathbf{cd})^{(m)} + (\mathbf{A} - \mathbf{B})_\mu(\mathbf{ab}|\mathbf{cd})^{(m)} \tag{50}$$

AUTHOR INFORMATION

Corresponding Author

*E-mail: xsli@uw.edu.

ORCID

Shichao Sun: 0000-0002-7680-3972
David B. Williams-Young: 0000-0003-2735-3706
Xiaosong Li: 0000-0001-7341-6240

Funding

The development of the two-component method is funded by the U.S. Department of Energy (DE-SC0006863). The development of nonperturbative spectroscopic methods is supported by the National Science Foundation (CHE-1565520). The development of the Chronus Quantum open source software package is supported by the National Science Foundation (OAC-1663636). D.W.-Y. was supported by a fellowship from The Molecular Sciences Software Institute (MolSSI) under NSF Grant ACI-1547580. Computations were facilitated through the use of advanced computational, storage, and networking infrastructure provided by the Hyak supercomputer system at the University of Washington, funded by the Student Technology Fee and the National Science Foundation (MRI-1624430).

Notes

The authors declare no competing financial interest.

REFERENCES

(1) Rigol, M.; Singh, R. R. P. Kagomé Lattice Antiferromagnets and Dzyaloshinsky-Moriya Interactions. *Phys. Rev. B: Condens. Matter Mater. Phys.* **2007**, *76*, 184403.

(2) Götze, O.; Farnell, D.; Bishop, R.; Li, P.; Richter, J. Heisenberg Antiferromagnet on the Kagomé Lattice With Arbitrary Spin: A Higher-order Coupled Cluster Treatment. *Phys. Rev. B: Condens. Matter Mater. Phys.* **2011**, *84*, 224428.

(3) Messio, L.; Bernu, B.; Lhuillier, C. Kagomé Antiferromagnet: A Chiral Topological Spin Liquid? *Phys. Rev. Lett.* **2012**, *108*, 207204.

(4) Mielke, A. Exact Ground States for the Hubbard Model on the Kagomé Lattice. *J. Phys. A: Math. Gen.* **1992**, *25*, 4335−4345.

(5) Helgaker, T.; Taylor, P. R. In *Modern Electronic Structure Theory*; Yarkony, D. R., Ed.; World Scientific Publishing Co. Pte. Ltd.: Singapore, 1995; Chapter 12, pp 725−856.

(6) Ding, F.; Liang, W.; Chapman, C. T.; Isborn, C. M.; Li, X. On the Gauge Invariance of Nonperturbative Electronic Dynamics Using the Time-Dependent Hartree-Fock and Time-Dependent Kohn-Sham. *J. Chem. Phys.* **2011**, *135*, 164101.

(7) Lestrange, P. J.; Egidi, F.; Li, X. The Consequences of Improperly Describing Oscillator Strengths Beyond the Electric Dipole Approximation. *J. Chem. Phys.* **2015**, *143*, 234103.

(8) Epstein, S. T. Gauge Invariance of the Hartree-Fock Approximation. *J. Chem. Phys.* **1965**, *42*, 2897−2898.

(9) Epstein, S. T. Gauge Invariance, Current Conservation, and GIAO's. *J. Chem. Phys.* **1973**, *58*, 1592−1595.

(10) Gauss, J.; Stanton, J. F. Electron-Correlated Approaches for the Calculation of NMR Chemical Shifts. *Adv. Chem. Phys.* **2003**, *123*, 355−422.

(11) Schindler, M.; Kutzelnigg, W. Theory of Magnetic Susceptibilities and NMR Chemical Shifts in Terms of Localized Quantities. II. Application to Some Simple Molecules. *J. Chem. Phys.* **1982**, *76*, 1919−1933.

(12) Kutzelnigg, W. Theory of Magnetic Susceptibilities and NMR Chemical Shifts in Terms of Localized Quantities. *Isr. J. Chem.* **1980**, *19*, 193−200.

(13) London, F. Théorie Quantique des Courants Interatomiques dans les Combinaisons Aromatiques. *J. Phys. Radium* **1937**, *8*, 397−409.

(14) Ditchfield, R. Molecular Orbital Theory of Magnetic Shielding and Magnetic Susceptibility. *J. Chem. Phys.* **1972**, *56*, 5688−5691.

(15) Wolinski, K.; Hinton, J. F.; Pulay, P. Efficient Implementation of the Gauge-Independent Atomic Orbital Method for NMR Chemical Shift Calculations. *J. Am. Chem. Soc.* **1990**, *112*, 8251−8260.

(16) Helgaker, T.; Jørgensen, P. An Electronic Hamiltonian for Origin Independent Calculations of Magnetic Properties. *J. Chem. Phys.* **1991**, *95*, 2595−2601.

(17) Bouten, R.; Baerends, E.; Van Lenthe, E.; Visscher, L.; Schreckenbach, G.; Ziegler, T. Relativistic Effects for NMR Shielding Constants in Transition Metal Oxides Using the Zeroth-Order Regular Approximation. *J. Phys. Chem. A* **2000**, *104*, 5600−5611.

(18) Krykunov, M.; Autschbach, J. Calculation of Origin-Independent Optical Rotation Tensor Components in Approximate Time-Dependent Density Functional Theory. *J. Chem. Phys.* **2006**, *125*, 034102.

(19) Autschbach, J. Analyzing NMR Shielding Tensors Calculated with Two-Component Relativistic Methods Using Spin-Free Localized Molecular Orbitals. *J. Chem. Phys.* **2008**, *128*, 164112.

(20) Helgaker, T.; Jaszuński, M.; Ruud, K. Ab Initio Methods for the Calculation of NMR Shielding and Indirect Spin-Spin Coupling Constants. *Chem. Rev.* **1999**, *99*, 293−352.

(21) Helgaker, T.; Coriani, S.; Jørgensen, P.; Kristensen, K.; Olsen, J.; Ruud, K. Recent Advances in Wave Function-Based Methods of Molecular-Property Calculations. *Chem. Rev.* **2012**, *112*, 543−631.

(22) Kappes, U.; Schmelcher, P. Electronic Bond Structure of the H_2^+ Ion in a Strong Magnetic Field: A Study of the Parallel Configuration. *Phys. Rev. A: At., Mol., Opt. Phys.* **1995**, *51*, 4542.

(23) Al-Hujaj, O.-A.; Schmelcher, P. Helium in Superstrong Magnetic Fields. *Phys. Rev. A: At., Mol., Opt. Phys.* **2003**, *67*, 023403.

(24) Kubo, A. The Hydrogen Molecule in Strong Magnetic Fields: Optimizations of Anisotropic Gaussian Basis Sets. *J. Phys. Chem. A* **2007**, *111*, 5572−5581.

(25) Tellgren, E. I.; Soncini, A.; Helgaker, T. Nonperturbative Ab Initio Calculations in Strong Magnetic Fields using London Orbitals. *J. Chem. Phys.* **2008**, *129*, 154114.

(26) Tellgren, E. I.; Helgaker, T.; Soncini, A. Non-Perturbative Magnetic Phenomena in Closed-Shell Paramagnetic Molecules. *Phys. Chem. Chem. Phys.* **2009**, *11*, 5489−5498.

(27) Stopkowicz, S.; Gauss, J.; Lange, K. K.; Tellgren, E. I.; Helgaker, T. Coupled-Cluster Theory for Atoms and Molecules in Strong Magnetic Fields. *J. Chem. Phys.* **2015**, *143*, 074110.

(28) Lange, K. K.; Tellgren, E. I.; Hoffmann, M.; Helgaker, T. A Paramagnetic Bonding Mechanism for Diatomics in Strong Magnetic Fields. *Science* **2012**, *337*, 327−331.

(29) Tellgren, E. I.; Teale, A. M.; Furness, J. W.; Lange, K.; Ekström, U.; Helgaker, T. Non-Perturbative Calculation of Molecular Magnetic Properties within Current-Density Functional Theory. *J. Chem. Phys.* **2014**, *140*, 034101.

(30) Furness, J. W.; Verbeke, J.; Tellgren, E. I.; Stopkowicz, S.; Ekström, U.; Helgaker, T.; Teale, A. M. Current Density Functional Theory Using Meta-Generalized Gradient Exchange-Correlation Functionals. *J. Chem. Theory Comput.* **2015**, *11*, 4169−4181.

(31) Furness, J. W.; Ekström, U.; Helgaker, T.; Teale, A. M. Electron Localisation Function in Current-Density-Functional Theory. *Mol. Phys.* **2016**, *114*, 1415−1422.

(32) Seeger, R.; Pople, J. A. Self-Consistent Molecular Orbital Methods. XVIII. Constraints and Stability in Hartree-Fock Theory. *J. Chem. Phys.* **1977**, *66*, 3045−3050.

(33) Anderson, P. W. *Basic Notions of Condensed Matter Physics*; Benjamin-Cummings, 1984.

(34) Fukutome, H. Unrestricted Hartree−Fock Theory and its Applications to Molecules and Chemical Reactions. *Int. J. Quantum Chem.* **1981**, *20*, 955−1065.

(35) Goings, J. J.; Ding, F.; Frisch, M. J.; Li, X. Stability of the Complex Generalized Hartree-Fock Equations. *J. Chem. Phys.* **2015**, *142*, 154109.

(36) Goings, J. J.; Egidi, F.; Li, X. Current Development of Non-collinear Electronic Structure Theory. *Int. J. Quantum Chem.* **2018**, *118*, No. e25398.

(37) Löwdin, P.-O.; Mayer, I. Some Studies of the General Hartree-Fock Method. *Adv. Quantum Chem.* **1992**, *24*, 79−114.

(38) Ding, F.; Goings, J. J.; Frisch, M. J.; Li, X. Ab Initio Non-Relativistic Spin Dynamics. *J. Chem. Phys.* **2014**, *141*, 214111.

(39) Ding, F.; Goings, J. J.; Liu, H.; Lingerfelt, D. B.; Li, X. Ab Initio Two-Component Ehrenfest Dynamics. *J. Chem. Phys.* **2015**, *143*, 114105.

(40) Sen, S.; Tellgren, E. I. Non-perturbative Calculation of Orbital and Spin Effects in Molecules Subject to Non-uniform Magnetic Fields. *J. Chem. Phys.* **2018**, *148*, 184112.

(41) Stuber, J. L.; Paldus, J. In *Fundamental World of Quantum Chemistry: A Tribute Vol. to the Memory of Per-Olov Löwdin*; Brändas, E. J., Kryachko, E. S., Eds.; Kluwer Academic Publishers, 2003; pp 67−139.

(42) Yamaki, D.; Shigeta, Y.; Yamanaka, S.; Nagao, H.; Yamaguchi, K. MP2, Tamm-Dancoff, and RPA Methods Based on the Generalized HF Solution. *Int. J. Quantum Chem.* **2000**, *80*, 701−707.

(43) Goings, J. J.; Ding, F.; Davidson, E. R.; Li, X. Approximate Singly Excited States from a Two-Component Hartree Fock Reference. *J. Chem. Phys.* **2015**, *143*, 144106.

(44) Kutzelnigg, W.; Liu, W. Quasirelativistic Theory Equivalent to Fully Relativistic Theory. *J. Chem. Phys.* **2005**, *123*, 241102.

(45) Liu, W.; Peng, D. Infinite-Order Quasirelativistic Density Functional Method Based on the Exact Matrix Quasirelativistic Theory. *J. Chem. Phys.* **2006**, *125*, 044102.

(46) Ilias, M.; Saue, T. An Infinite-Order Relativistic Hamiltonian by a Simple One-Step Transformation. *J. Chem. Phys.* **2007**, *126*, 064102.

(47) Liu, W.; Peng, D. Exact Two-component Hamiltonians Revisited. *J. Chem. Phys.* **2009**, *131*, 031104.

(48) Peng, D.; Middendorf, N.; Weigend, F.; Reiher, M. An Efficient Implementation of Two-Component Relativistic Exact-Decoupling Methods for Large Molecules. *J. Chem. Phys.* **2013**, *138*, 184105.

(49) Peng, D.; Liu, W.; Xiao, Y.; Cheng, L. Making Four- and Two-Component Relativistic Density Functional Methods Fully Equivalent Based on the Idea of From Atoms to Molecule. *J. Chem. Phys.* **2007**, *127*, 104106.

(50) Egidi, F.; Goings, J. J.; Frisch, M. J.; Li, X. Direct Atomic-Orbital-Based Relativistic Two-Component Linear Response Method for Calculating Excited-State Fine Structures. *J. Chem. Theory Comput.* **2016**, *12*, 3711−3718.

(51) Williams-Young, D.; Egidi, F.; Li, X. Relativistic Two-Component Particle-Particle Tamm-Dancoff Approximation. *J. Chem. Theory Comput.* **2016**, *12*, 5379−5384.

(52) Egidi, F.; Sun, S.; Goings, J. J.; Scalmani, G.; Frisch, M. J.; Li, X. Two-Component Non-Collinear Time-Dependent Spin Density Functional Theory for Excited State Calculations. *J. Chem. Theory Comput.* **2017**, *13*, 2591−2603.

(53) Petrone, A.; Williams-Young, D. B.; Sun, S.; Stetina, T. F.; Li, X. An Efficient Implementation of Two-Component Relativistic Density Functional Theory with Torque-Free Auxiliary Variables. *Eur. Phys. J. B* **2018**, *91*, 169.

(54) Pople, J. Molecular-Orbital Theory of Diamagnetism. I. An Approximate LCAO Scheme. *J. Chem. Phys.* **1962**, *37*, 53−59.

(55) Hameka, H. Calculation of Magnetic Susceptibilities of Diatomic Molecules: I. General Theory. *Physica* **1962**, *28*, 908−916.

(56) Hameka, H. On Pople's Molecular-Orbital Theory of Diamagnetism. *J. Chem. Phys.* **1962**, *37*, 3008−3009.

(57) Pople, J. Reply to Letter by HF Hameka. *J. Chem. Phys.* **1962**, *37*, 3009−3010.

(58) Li, X.; Valeev, E.; Williams-Young, D.; Petrone, A.; Sun, S.; Stetina, T.; Wildman, A.; Goings, J.; Kasper, J.; Ding, F.; Lestrange, P. *Chronus Quantum*, Beta 0.2 version. http://www.chronusquantum.org (2018).

(59) Dunning, T. H., Jr Gaussian Basis Sets for Use in Correlated Molecular Calculations. I. The Atoms Boron through Neon and Hydrogen. *J. Chem. Phys.* **1989**, *90*, 1007−1023.

(60) Li, X.; Frisch, M. J. Energy-Represented Direct Inversion in the Iterative Subspace within a Hybrid Geometry Optimization Method. *J. Chem. Theory Comput.* **2006**, *2*, 835−839.

(61) Frisch, M. J.; Trucks, G. W.; Schlegel, H. B.; Scuseria, G. E.; Robb, M. A.; Cheeseman, J. R.; Scalmani, G.; Barone, V.; Petersson, G. A.; Nakatsuji, H.; Li, X.; Caricato, M.; Marenich, A. V.; Bloino, J.; Janesko, B. G.; Gomperts, R.; Mennucci, B.; Hratchian, H. P.; Ortiz, J. V.; Izmaylov, A. F.; Sonnenberg, J. L.; Williams-Young, D.; Ding, F.; Lipparini, F.; Egidi, F.; Goings, J.; Peng, B.; Petrone, A.; Henderson, T.; Ranasinghe, D.; Zakrzewski, V. G.; Gao, J.; Rega, N.; Zheng, G.; Liang, W.; Hada, M.; Ehara, M.; Toyota, K.; Fukuda, R.; Hasegawa, J.; Ishida, M.; Nakajima, T.; Honda, Y.; Kitao, O.; Nakai, H.; Vreven, T.; Throssell, K.; Montgomery, J. A., Jr.; Peralta, J. E.; Ogliaro, F.; Bearpark, M. J.; Heyd, J. J.; Brothers, E. N.; Kudin, K. N.; Staroverov, V. N.; Keith, T. A.; Kobayashi, R.; Normand, J.; Raghavachari, K.; Rendell, A. P.; Burant, J. C.; Iyengar, S. S.; Tomasi, J.; Cossi, M.; Millam, J. M.; Klene, M.; Adamo, C.; Cammi, R.; Ochterski, J. W.; Martin, R. L.; Morokuma, K.; Farkas, O.; Foresman, J. B.; Fox, D. J. *Gaussian 16*, revision A.03; Gaussian Inc.: Wallingford, CT, 2016.

(62) Becke, A. D. Density-Functional Thermochemistry. III. The Role of Exact Exchange. *J. Chem. Phys.* **1993**, *98*, 5648−5652.

(63) Lee, C.; Yang, W.; Parr, R. G. Development of the Colle-Salvetti Correlation-Energy Formula into a Functional of the Electron Density. *Phys. Rev. B: Condens. Matter Mater. Phys.* **1988**, *37*, 785.

(64) Vosko, S. H.; Wilk, L.; Nusair, M. Accurate Spin-Dependent Electron Liquid Correlation Energies for Local Spin Density Calculations. *Can. J. Phys.* **1980**, *58*, 1200−1211.

(65) Stephens, P.; Devlin, F.; Chabalowski, C.; Frisch, M. J. Ab Initio Calculation of Vibrational Absorption and Circular Dichroism Spectra Using Density Functional Force Fields. *J. Phys. Chem.* **1994**, *98*, 11623−11627.

(66) Goodenough, J. *Magnetism and the Chemical Bond*; John Wiley & Sons, 1963.

(67) Decurtins, S.; Guedel, H. U.; Pfeuti, A. Optical Spectroscopy of $[(NH_3)_4Cr(OH)_2Cr(NH3)_4]^{4+}$ and $[(en)_2Cr(OH)_2Cr(en)_2]^{4+}$. *Inorg. Chem.* **1982**, *21*, 1101−1106.

(68) Decurtins, S.; Guedel, H. U. Superexchange in Bis(μ-hydroxo)-Bridged Chromium(III) Dimers. Optical Spectroscopic Study of Singly Excited $^2E_g{}^4A^{2g}$ pair states. *Inorg. Chem.* **1982**, *21*, 3598−3606.

(69) Honda, M.; Sato, K.; Obara, S. Formulation of Molecular Integrals over Gaussian Functions Treatable by both the Laplace and Fourier Transforms of Spatial Operators by Using Derivative of Fourier-Kernel Multiplied Gaussians. *J. Chem. Phys.* **1991**, *94*, 3790−3804.

(70) Irons, T. J.; Zemen, J.; Teale, A. M. Efficient Calculation of Molecular Integrals over London Atomic Orbitals. *J. Chem. Theory Comput.* **2017**, *13*, 3636−3649.

(71) Head-Gordon, M.; Pople, J. A. A Method for Two-Electron Gaussian Integral and Integral Derivative Evaluation Using Recurrence Relations. *J. Chem. Phys.* **1988**, *89*, 5777−5786.

NOTE ADDED AFTER ASAP PUBLICATION

This paper was published ASAP on December 13, 2018, with errors in equations 47 and 50. The corrected version was reposted December 18, 2018.